16th European Signal Processing Conference (EUSIPCO 2008), Lausanne, Switzerland, August 25-29, 2008, copyright by EURASIP

ON PHASE STATISTICS OF COMPLEX WAVELET COEFFICIENTS AT EDGES

Yothin Rakvongthai and Soontorn Oraintara

Department of Electrical Engineering, University of Texas Arlington
Arlington, TX 76019 USA
Email: rakvongthai@msp.uta.edu, oraintar@uta.edu
Web: www-ee.uta.edu/msp

ABSTRACT

We investigate the phase information in the dual-tree complex wavelet transform (DT-ℂWT) framework. The probability density function (pdf) of the phase of a complex wavelet coefficient is derived for the edge-type input. A simple method to estimate the parameters of the pdf is presented. The simulation results confirm that the results are consistent with the actual coefficients for both synthetic input and natural images.

1. INTRODUCTION

The importance of phase in signal processing has been known for a long time. One of the classical illustrations is shown in [1], where the image reconstruction is dominated by the phase of the Fourier transform of an image rather than by the magnitude of the transform. The edge features are very crucial in human visual perception [2]. Moreover, singularity features (e.g. edges) have been found to be closely related to the phase of signals.

There have been research studies on using phase information of the complex wavelet transform. In [3, 4], it is observed that, in each scale, the phase of a coefficient near an isolated feature varies linearly with its distance to the feature. This observation is then utilized for feature orientation determination [3], and object recognition [4, 5]. In [6], a proof of this linear relation is given and employed for texture image retrieval using a complex directional transform. Moreover, the phase information of the complex coefficients is also used for feature detection [7, 8]. In [9], the orientation and the offset of a coefficient to an edge in an image are shown to be related to the phase as well as the magnitude of the coefficient, which is used to generate a geometrical Hidden Markov tree (GHMT) model. In [10], the interscale relationship and prediction of the complex wavelet phases are presented, and used to hypothesize that humans percept the blur when local phase coherence is not met. Another interscale phase relationship is investigated and used in image modeling and denoising [11, 12]. Furthermore, in [13, 14], a similar interscale phase relationship is proposed and incorporated to generate a hidden Markov tree (HMT) model. In that proposed HMT model, the phase of the coefficients near an edge is claimed to have the symmetric Beta distribution since it is densely distributed around a particular value. Recently in [15], the pdf of the derotated phase of complex wavelet coefficients has been determined, and found to be well approximated by the Gaussian pdf when the variance is small. However, the phase pdf of a coefficient at an edge has not been clarified yet.

Based on the dual-tree complex wavelet transform (DT-ℂWT) [16], in this work we propose an edge model and derive the phase pdf of a complex coefficient at an edge. A simple parameter estimation method for the derived pdf is presented. Note that the results of the phase pdf also apply to other complex wavelet transforms, not just the DT-ℂWT.

2. PRELIMINARIES

2.1 The dual-tree complex wavelet transform

The DT-ℂWT [16] consists of two trees of filter banks: the real and the imaginary trees, which provide the real and the imaginary parts of the coefficients, respectively. It possesses nice properties such as nearly shift invariance, good directional selectivity, and considerably low redundancy. Let $x[n]$ be the input of the DT-ℂWT shown in Fig.1, and let $\{H_0^{(1)}(e^{j\omega}), H_1^{(1)}(e^{j\omega}); G_0^{(1)}(e^{j\omega}), G_1^{(1)}(e^{j\omega})\}$ be the dual-tree filter pairs (in the frequency domain) for the real and imaginary trees for the first scale, and $\{H_0(e^{j\omega}), H_1(e^{j\omega}); G_0(e^{j\omega}), G_1(e^{j\omega})\}$ be the dual-tree filter pairs for the succeeding scales. Let $c_i[n] = a_i[n] + jb_i[n]$ be the complex coefficients in scale i. To have those nice properties as mentioned earlier, the wavelet functions of the DT-ℂWT should be analytic. For the DT-ℂWT to be analytic, the lowpass filters should be chosen such that [17]

$$G_0^{(1)}(e^{j\omega}) = e^{-j\omega} H_0^{(1)}(e^{j\omega}), \quad (1)$$

$$\text{and} \quad G_0(e^{j\omega}) = e^{-j\theta(\omega)} H_0(e^{j\omega}), \quad (2)$$

where $\theta(\omega) = \frac{\omega}{2}$ when $|\omega| < \pi$ and $\theta(\omega) = \theta(\omega + 2\pi)$. Note that the half-sample delay condition (2) is sufficient and necessary for the corresponding wavelet functions $\psi_h(t)$ (for the real part) and $\psi_g(t)$ (for the imaginary part) to form a Hilbert transform pair [18], i.e., $\Psi_g(\omega) = -\text{sgn}(\omega) j \Psi_h(\omega)$, which implies that in each scale the corresponding filters in real and imaginary trees of the DT-ℂWT form a Hilbert transform pair [19]. We refer to [16, 17] for more details on the DT-ℂWT.

2.2 The phase pdf of complex random variables

In this subsection, we will discuss the phase pdf of a complex random variable where its real and imaginary parts are Gaussian random variables.

Let X and Y be two zero-mean Gaussian random variables with variances σ_1^2 and σ_2^2, respectively. The joint pdf between X and Y is [20]

$$f_{X,Y}(x,y) = \frac{e^{-\left[\frac{1}{2(1-\rho^2)}\left(\frac{x^2}{\sigma_1^2} - \frac{2\rho xy}{\sigma_1\sigma_2} + \frac{y^2}{\sigma_2^2}\right)\right]}}{2\pi\sigma_1\sigma_2\sqrt{1-\rho^2}},$$

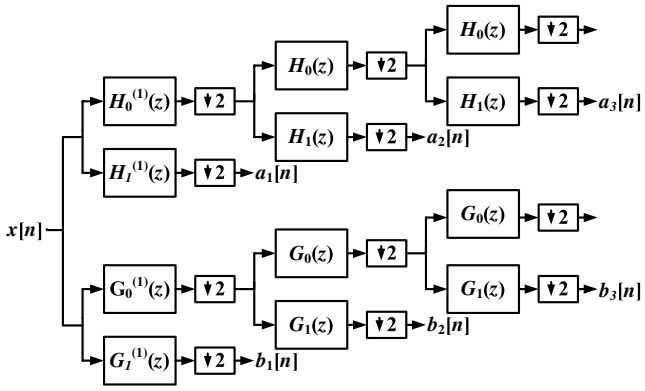

Figure 1: The first three scales of the analysis filter bank for the DT-$\mathbb{C}$WT

where ρ is the correlation coefficient between X and Y. Making the change of variables $x = r\cos\theta$, $y = r\sin\theta$ with $r \geq 0$ and $-\pi \leq \theta < \pi$, we obtain the joint pdf of random variables R and Θ as

$$f_{R,\Theta}(r,\theta) = \frac{re^{-\left[\frac{r^2}{2(1-\rho^2)}\left(\frac{\cos^2\theta}{\sigma_1^2} - \frac{\rho\sin 2\theta}{\sigma_1\sigma_2} + \frac{\sin^2\theta}{\sigma_2^2}\right)\right]}}{2\pi\sigma_1\sigma_2\sqrt{1-\rho^2}}.$$

Let $\sigma^2 = \sigma_1^2 + \sigma_2^2$, $\eta = \frac{1}{\sigma^2}\sqrt{(\sigma_1^2-\sigma_2^2)^2 + 4\rho^2\sigma_1^2\sigma_2^2}$, and $\gamma = \text{atan2}(2\rho\sigma_1\sigma_2, \sigma_1^2-\sigma_2^2)$, where

$$\text{atan2}(y,x) \triangleq \angle(x+jy) = \begin{cases} \tan^{-1}(\frac{y}{x}), & \text{if } x \geq 0; \\ \tan^{-1}(\frac{y}{x}) + \pi, & \text{if } x < 0,\ y \geq 0; \\ \tan^{-1}(\frac{y}{x}) - \pi, & \text{if } x < 0,\ y < 0. \end{cases}$$

Note that $0 \leq \eta \leq 1$ and $-\pi \leq \gamma < \pi$. Then, we have

$$f_{R,\Theta}(r,\theta) = \frac{r}{\pi\sigma^2\sqrt{1-\eta^2}}\, e^{-\left[\frac{r^2(1-\eta\cos(2\theta-\gamma))}{\sigma^2(1-\eta^2)}\right]}.$$

With the aid of the modified Bessel function of the first kind and zeroth order defined as [20] $I_0(z) \triangleq \frac{1}{2\pi}\int_0^{2\pi} e^{z\cos\theta}d\theta$, the marginal pdf of R is given by

$$f_R(r) = \frac{2r}{\sigma^2\sqrt{1-\eta^2}}\, e^{-\frac{r^2}{\sigma^2(1-\eta^2)}} I_0\left(\frac{r^2\eta}{\sigma^2(1-\eta^2)}\right). \quad (3)$$

On the other hand, the marginal pdf of Θ is obtained by

$$f_\Theta(\theta) = \frac{\sqrt{1-\eta^2}}{2\pi(1-\eta\cos(2\theta-\gamma))}. \quad (4)$$

Using (3) and (4), we can find the magnitude and phase pdf's of the complex random variable which is herein the complex coefficient. In this paper, we will focus exclusively on the phase pdf.

3. THE PHASE PDF AT ISOLATED EDGES

The goal of this section is to propose the phase pdf of a complex coefficient when the input is an edge. To find the phase pdf of a coefficient at an edge accurately, we need a realistic edge model. In this paper, we model an edge as a step signal corrupted by an additive white Gaussian noise, where the amplitude of the step A is a zero-mean Gaussian random variable. Without loss of generality, we assume that the edge is present at $n = 0$. Hence, the mathematical model of the edge is

$$x[n] = A\mu[n] + w[n], \quad (5)$$

where $A \sim \mathcal{N}(0,\sigma_E^2)$, $\mu[n]$ is the unit step signal defined by

$$\mu[n] = \begin{cases} 1, & n \geq 0; \\ 0, & n < 0, \end{cases}$$

and $w[n] \sim \mathcal{N}(0,\sigma_w^2)$ is uncorrelated to A. Let $\alpha_i + j\beta_i$ be the complex coefficient due to the unit step signal $\mu[n]$, and $u_i + jv_i$ be the complex coefficient due to the noise $w[n]$, all in scale i at the edge location. Then, we have $\alpha_i = \sum_k \text{Re}\{h_i[k]\}\mu[-k]$, $\beta_i = \sum_k \text{Im}\{h_i[k]\}\mu[-k]$, $u_i = \sum_k \text{Re}\{h_i[k]\}w[-k]$, and $v_i = \sum_k \text{Im}\{h_i[k]\}w[-k]$ for some corresponding complex filter $h_i[k]$. Similarly, we can assume that $E[u_i] = E[v_i] = 0$. Let $\sigma_{u_i}^2$, $\sigma_{v_i}^2$, and λ_i be the variances of u_i and v_i, and their correlation coefficient respectively. Then, we obtain

$$\begin{aligned} \sigma_{u_i}^2 &= E[\sum_{k_1}\text{Re}\{h_i[k_1]\}w[-k_1]\sum_{k_2}\text{Re}\{h_i[k_2]\}w[-k_2]] \\ &= \sum_{k_1}\sum_{k_2}\text{Re}\{h_i[k_1]\}\text{Re}\{h_i[k_2]\}E[w[-k_1]w[-k_2]] \\ &= \sum_{k_1}\sum_{k_2}\text{Re}\{h_i[k_1]\}\text{Re}\{h_i[k_2]\}\sigma_w^2\delta[k_1-k_2] \\ &= \sigma_w^2\sum_k(\text{Re}\{h_i[k]\})^2. \end{aligned}$$

Similarly, we have $\sigma_{v_i}^2 = \sigma_w^2\sum_k(\text{Im}\{h_i[k]\})^2$. Thanks to the relationships between the filters in (1) and (2), we have

$$\sum_k(\text{Re}\{h_i[k]\})^2 = \sum_k(\text{Im}\{h_i[k]\})^2 \triangleq K_i, \quad (6)$$

and hence $\sigma_{u_i}^2 = \sigma_{v_i}^2$. Moreover, we obtain their correlation coefficient as

$$\begin{aligned} \lambda_i &= \frac{E[\sum_{k_1}\text{Re}\{h_i[k_1]\}w[-k_1]\sum_{k_2}\text{Im}\{h_i[k_2]\}w[-k_2]]}{\sigma_{u_i}\sigma_{v_i}} \\ &= \sigma_w^2\sum_k\text{Re}\{h_i[k]\}\text{Im}\{h_i[k]\}/(\sigma_{u_i}\sigma_{v_i}) \\ &= \frac{\sigma_w^2 L_i}{\sigma_{u_i}\sigma_{v_i}}, \text{ where } L_i \triangleq \sum_k\text{Re}\{h_i[k]\}\text{Im}\{h_i[k]\}. \end{aligned}$$

Since in scale $i > 1$ the real and imaginary parts of the corresponding complex filter h_i form a Hilbert transform pair, they are orthogonal. Then, we obtain that $L_i = 0$ for $i \geq 2$. Since $w[n]$ and A are uncorrelated, both u_i and v_i are uncorrelated to A. Due to the linearity of the DT-$\mathbb{C}$WT, the complex coefficient at the edge in scale i, c_i, is given by $c_i = a_i + jb_i = (A\alpha_i + u_i) + j(A\beta_i + v_i)$. Hence, the mean and variance of a_i and b_i are $E[a_i] = E[b_i] = 0$, $\sigma_{a_i}^2 = \alpha_i^2\sigma_E^2 + \sigma_{u_i}^2$ and $\sigma_{b_i}^2 = \beta_i^2\sigma_E^2 + \sigma_{v_i}^2$, respectively. The correlation coefficient between a_i and b_i is obtained by

$$\rho_i = \frac{E[a_ib_i]}{\sigma_{a_i}\sigma_{b_i}} = \frac{\alpha_i\beta_i\sigma_E^2 + \lambda_i\sigma_{u_i}\sigma_{v_i}}{\sigma_{a_i}\sigma_{b_i}} = \frac{\alpha_i\beta_i\sigma_E^2 + \sigma_w^2 L_i}{\sigma_{a_i}\sigma_{b_i}}.$$

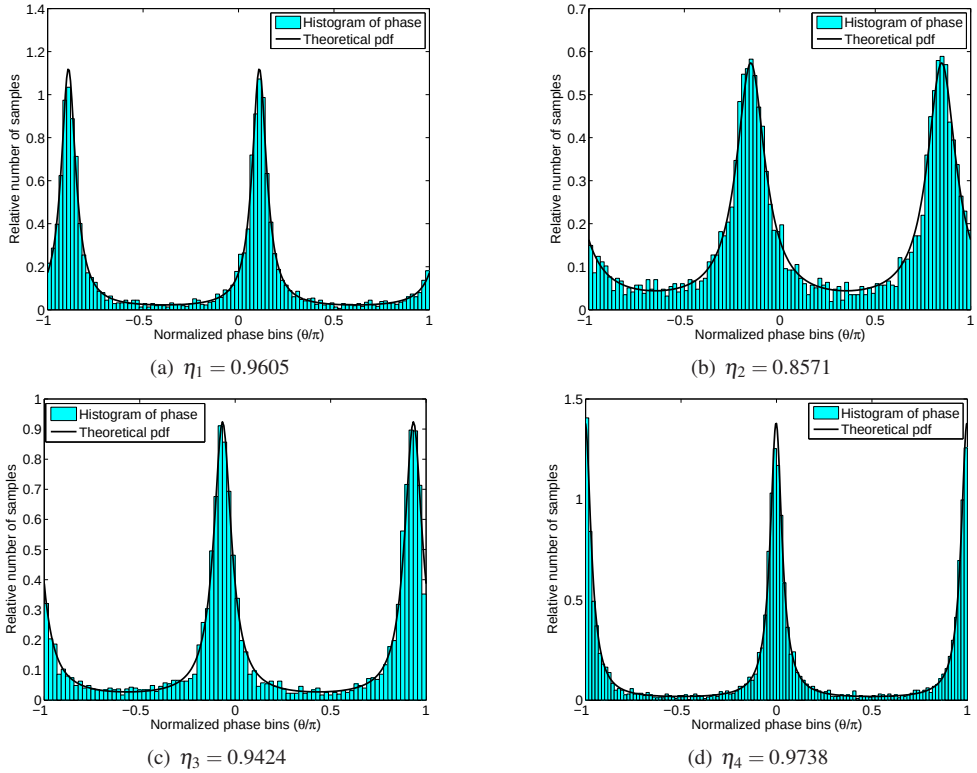

(a) $\eta_1 = 0.9605$ (b) $\eta_2 = 0.8571$

(c) $\eta_3 = 0.9424$ (d) $\eta_4 = 0.9738$

Figure 2: At the edge: the histograms and the theoretical phase pdf's (a) in scale 1, (b) in scale 2, (c) in scale 3, and (d) in scale 4.

Let $\sigma_i^2 = \sigma_{a_i}^2 + \sigma_{b_i}^2$, $\eta_i = \frac{1}{\sigma_i^2}\sqrt{(\sigma_{a_i}^2 - \sigma_{b_i}^2)^2 + 4\rho_i^2\sigma_{a_i}^2\sigma_{b_i}^2}$, and $\gamma_i = \text{atan2}(2\rho_i\sigma_{a_i}\sigma_{b_i}, \sigma_{a_i}^2 - \sigma_{b_i}^2)$. Therefore, we can write η_i and γ_i as

$$\begin{aligned} \eta_i &= \frac{\sqrt{\kappa^2(\alpha_i^2 - \beta_i^2)^2 + 4(\alpha_i\beta_i\kappa + L_i)^2}}{\kappa(\alpha_i^2 + \beta_i^2) + 2K_i}, \\ \gamma_i &= \text{atan2}\big(2(\alpha_i\beta_i\kappa + L_i), \kappa(\alpha_i^2 - \beta_i^2)\big), \end{aligned}$$

where $\kappa = \sigma_E^2/\sigma_w^2$. Accordingly, from (4), the phase pdf can be obtained by

$$f_{\angle c_i}(\theta) = \frac{\sqrt{1-\eta_i^2}}{2\pi(1 - \eta_i\cos(2\theta - \gamma_i))}. \qquad (7)$$

The histograms and the theoretical phase pdf's of the complex coefficient at the edge in scales 1-4 with $\sigma_E^2 = 1$ and $\sigma_w^2 = 0.01$ are shown in Figs. 2(a)-2(d). It can be seen that the phase histograms fit well with the pdf derived in (7). From Table 1, one can see that for $i \geq 2$ the parameter η_i increases as i increases, i.e. the phase is more densely distributed around two particular values as we increase i. This is because the magnitude of the complex coefficient at the edge increases as we increase the scale i. Nevertheless, the parameter in scale 1, η_1, does not correspond to this trend because of the difference between the filters in the first and other scales. As examples for natural images, the edges, the histograms, and the phase pdf's of complex coefficients at edges in scale 1 for the slices of "Lena", "Man", and "Boat" images are shown in Figs. 3(a)-3(l). We show the phase histograms of the coefficients at edges for two directions:

Table 1: Parameter η in scales 1, 2, 3, and 4

Scale i	1	2	3	4
η	0.9605	0.8571	0.9424	0.9738

Table 2: Parameter Estimation Error

Scale i	$\hat{\eta}/\eta$	Error
1	$0.9715/0.9605$	1.15%
2	$0.8929/0.8571$	4.14%
3	$0.9530/0.9424$	1.12%
4	$0.9726/0.9738$	0.12%
Scale i	$\hat{\gamma}/\gamma$	Error
1	$0.2162\pi/0.2186\pi$	0.0024π
2	$-0.3007\pi/-0.3037\pi$	0.0030π
3	$-0.1377\pi/-0.1321\pi$	0.0056π
4	$-0.0061\pi/-0.0036\pi$	0.0025π

vertical and horizontal directions, which correspond to the slices along the rows and along the columns respectively. The edges in each direction are determined from the edges of the image which are found using Canny edge detection method [21]. As can be observed, the pdf's which are found by curve fitting correspond to the histograms for all three images in both horizontal and vertical edge directions.

4. THE TWO PARAMETERS OF THE PHASE PDF

The phase pdf (4) is characterized by the two parameters γ and η. The parameter γ indicates the values of θ which maximize (and minimize) $f_\Theta(\theta)$, while the parameter η indicates how sharp the pdf is, i.e. how close the pdf is to the uniform distribution. The less the value of η is, the closer the pdf becomes the uniform distribution. Next, we will give a simple method to estimate the two parameters.

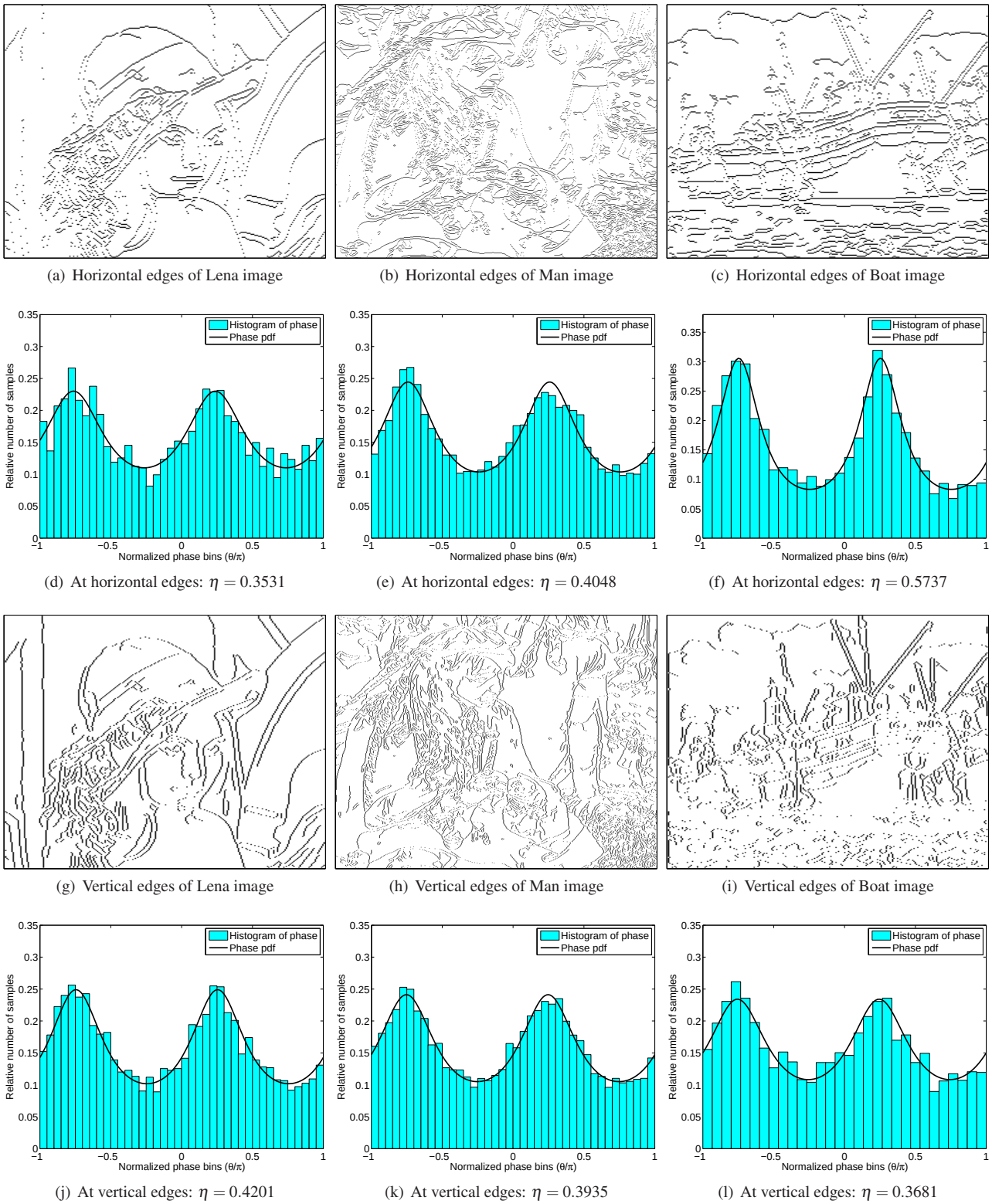

(a) Horizontal edges of Lena image (b) Horizontal edges of Man image (c) Horizontal edges of Boat image

(d) At horizontal edges: $\eta = 0.3531$ (e) At horizontal edges: $\eta = 0.4048$ (f) At horizontal edges: $\eta = 0.5737$

(g) Vertical edges of Lena image (h) Vertical edges of Man image (i) Vertical edges of Boat image

(j) At vertical edges: $\eta = 0.4201$ (k) At vertical edges: $\eta = 0.3935$ (l) At vertical edges: $\eta = 0.3681$

Figure 3: Phase pdf of a coefficient at edges in natural images: Lena image, (a) horizontal edges, (d) the histogram and phase pdf in scale 1 at horizontal edges, (g) vertical edges, (j) histograms and phase pdf in scale 1 at vertical edges; Man image, (b) horizontal edges, (e) the histogram and phase pdf in scale 1 at horizontal edges, (h) vertical edges, (k) histograms and phase pdf in scale 1 at vertical edges; Boat image, (c) horizontal edges, (f) the histogram and phase pdf in scale 1 at horizontal edges, (i) vertical edges, (l) histograms and phase pdf in scale 1 at vertical edges. In each edge image, an edge pixel is represented by black color.

Let $\theta_{\max} = \arg\max_\theta f_\Theta(\theta)$, and $\theta_{\min} = \arg\min_\theta f_\Theta(\theta)$. It is easy to see that

$$\theta_{\max} = \gamma/2 \text{ and } \begin{cases} \gamma/2+\pi, & \text{if } \gamma < 0; \\ \gamma/2-\pi, & \text{if } \gamma > 0. \end{cases}$$

Due to symmetry of the pdf, we obtain

$$\theta_{\min} = \gamma/2+\pi/2 \text{ and } \gamma/2-\pi/2.$$

For parameter estimation, we propose $\hat{\gamma}$, the estimate of γ, as

$$\hat{\gamma} = \text{atan2}\left(\sum_k \sin(2\theta_k), \sum_k \cos(2\theta_k)\right),$$

which is the circular mean of $2\theta_k$. On the other hand, since the maximum and the minimum of $f_\Theta(\theta)$ are $f_{\max} = \frac{\sqrt{1-\eta^2}}{2\pi(1-\eta)}$ and $f_{\min} = \frac{\sqrt{1-\eta^2}}{2\pi(1+\eta)}$, we propose the estimate $\hat{\eta}$ for η to be

$$\hat{\eta} = \frac{\lambda-1}{\lambda+1},$$

where $\lambda = \frac{f_{\max}}{f_{\min}}$, whose approximated value can be found from the data histogram. Table 2 shows the estimation error for the two parameters in the first four scales ($i = 1,\ldots,4$). It can be seen that the estimation error for both parameters is acceptable while the estimation method is simple.

5. CONCLUSION

We have statistically modeled the phase of a complex coefficient in the dual-tree complex wavelet transform (DT-$\mathbb{C}$WT) framework. The edge model has been proposed and the phase pdf of a coefficient at edges has been derived. The simulation results are provided to confirm the correctness of the derived pdf. Although we herein consider in the DT-$\mathbb{C}$WT framework, the results obtained also apply to other complex wavelet transforms. Moreover, a simple parameter estimation method for the pdf is also provided. The method gives a satisfying result in spite of its simplicity.

REFERENCES

[1] A.V. Oppenheim and J.S. Lim, "The importance of phase in signals," in *Proc. of the IEEE*, May 1981, vol. 69, pp. 529–541.

[2] D. Marr, *Vision: A Computational Investigation into the Human Representation and Processing of Visual Information*, W. H. Freeman, San Francisco, CA, 1982.

[3] R. Anderson, N. Kingsbury, and J. Fauqueur, "Determining multiscale image feature angles from complex wavelet phases," in *Proc. ICIAR 2005*, Toronto, Canada, September 28-30. 2005.

[4] R. Anderson, N. Kingsbury, and J. Fauqueur, "Coarse level object recognition using interlevel products of complex wavelets," in *Proc. IEEE ICASSP 2005*, Philadelphia, PA, March 18-23. 2005, vol. 1, pp. I–745–748.

[5] R. Anderson, N. Kingsbury, and J. Fauqueur, "Rotation-invariant object recognition using edge profile clusters," in *Proc. EUSIPCO 2006*, Florence, Italy, September 4-8. 2006.

[6] A.P.N. Vo, S. Oraintara, and T.T. Nguyen, "Using phase and magnitude information of the complex directional filter bank for texture image retrieval," in *Proc. IEEE ICIP 2007*, San Antonio, TX, September 16-19. 2007, vol. 4, pp. IV–61–64.

[7] P.D. Kovesi, "Image features from phase congruency," *J. Comput. Vis. Res.*, vol. 16, no. 3, Summer 1999.

[8] N. Kingsbury, "Rotation-invariant local feature matching with complex wavelets," in *Proc. EUSIPCO 2006*, Florence, Italy, September 4-8. 2006.

[9] J.K. Romberg, M.B. Wakin, H. Choi, and R.G. Baraniuk, "A geometric hidden markov tree wavelet model," in *Proc. Wavelet Applications Signal Image Processing X (SPIE 5207)*, 2003, pp. 80–86.

[10] Z. Wang and E.P. Simoncelli, "Local phase coherence and the perception of blur," in *Adv. Neural Information Processing Systems (NIPS03)*, Cambridge, MA, May 2004, vol. 16, MIT Press.

[11] M. Miller and N. Kingsbury, "Image estimation using interscale phase properties of complex wavelet coefficients," *IEEE Trans. Image Process.*, "Accepted for publication".

[12] M. Miller and N. Kingsbury, "Image denoising using derotated complex wavelet coefficients," *IEEE Trans. Image Process.*, "Accepted for publication".

[13] J.K. Romberg, H. Choi, and R.G. Baraniuk, "Multiscale edge grammars for complex wavelet transforms," in *Proc. IEEE ICIP 2001*, Thessaloniki, Greece, October 7-10. 2001, vol. 1, pp. 614–617.

[14] J.K. Romberg, M.B. Wakin, H. Choi, N.G. Kingsbury, and R.G. Baraniuk, "A hidden markov tree model for the complex wavelet transform," Tech. Rep., Rice Univ., 2002.

[15] Y. Rakvongthai and S. Oraintara, "On the probability density function of the derotated phase of complex wavelet coefficients," in *Proc. IEEE ISCAS 2008*, Seattle, WA (to appear).

[16] N.G. Kingsbury, "Complex Wavelets for shift invariant analysis and filtering of signals," *Applied Computat. Harmon. Anal.*, pp. 234–253, May. 2001.

[17] I.W. Selesnick, R.G. Baranuik, and N.G. Kingsbury, "The dual-tree complex wavelet transform," *IEEE Signal Process. Mag.*, vol. 22, pp. 123–151, Nov. 2005.

[18] H. Ozkaramanli and R. Yu, "On the phase condition and its solution for hilbert transform pairs of wavelet bases," *IEEE Trans. Signal Process.*, vol. 51, pp. 3293–3294, Dec. 2003.

[19] J.H. Won, K. Pyun, and R.M. Gray, "Hidden markov multiresolution texture segmentation using complex wavelets," in *Proc. IEEE ICT 2003*, Tahiti, French Polynesia, February 23-March 1. 2003, vol. 2, pp. 1624–1630.

[20] A. Papoulis and S.U. Pillai, *Probability, Random Variables and Stochastic Processes*, McGraw-Hill, New York, NY, 2002.

[21] J. Canny, " A computational approach to edge detection," *IEEE Trans. Pattern Anal. Machine Intell.*, vol. PAMI-8, No. 6, 1986, pp. 679-698.